CrystEngComm

PAPER

View Article Online
View Journal | View Issue

Cite this: *CrystEngComm*, 2017, **19**, 1389

Chelate ring stacking interactions in the supramolecular assemblies of Zn(II) and Cd(II) coordination compounds: a combined experimental and theoretical study†

Farhad Akbari Afkhami,[a] Ali Akbar Khandar,*[a] Ghodrat Mahmoudi,*[b] Waldemar Maniukiewicz,[c] Atash V. Gurbanov,[de] Fedor I. Zubkov,[e] Onur Şahin,[f] Okan Zafer Yesilel[g] and Antonio Frontera*[h]

Received 30th December 2016,
Accepted 7th February 2017

DOI: 10.1039/c6ce02666d

rsc.li/crystengcomm

The self-assembly of Zn(II) and Cd(II) ions with two isomeric tetradentate ligands, 2-pyridyl-isonicotinoylhydrazone (HL^1) and 2-benzoylpyridyl-picolinoylhydrazone (HL^2), was studied by elemental analysis, FT-IR spectroscopy and single-crystal X-ray diffraction. The reaction of zinc(II) and cadmium(II) salts with HL^1 and HL^2 in methanol under solvothermal conditions produced six monomer and one tetranuclear zinc(II) complexes, namely, $Zn(HL^1)Br_2$ (**1**), $Zn(HL^1)Cl_2$ (**2**), $[Cd(HL^1)_2](NO_3)_2{\cdot}H_2O$ (**3**), $Cd(HL^2)Br_2$(**4**), $Zn(HL^2)Cl_2$ (**5**), $Zn(HL^2)Br_2$ (**6**) and $[Zn_4(L^2)_4I_2][ZnI_4]{\cdot}2H_2O$ (**7**). The structure of **7** includes a cationic tetranuclear cluster of four zinc ions, four ligands, and two anions, counterbalanced by ZnI_4^{2-} ions. However, the reaction of zinc(II) and cadmium(II) salts with HL^1 under the same conditions produced monomer compounds. Herein, the ligand effects on the complex structures were studied. Hirshfeld surface analysis and fingerprint plots facilitate the comparison of intermolecular interactions in compounds **1**–**7**, which are crucial in building supramolecular architectures.

Introduction

Molecular clusters have received significant attention owing to their structural diversity resulting from their metal-rich nature and chemical stability combined with their fascinating potential application in advanced materials.[1–3] An increasing number of geometrically intriguing molecular clusters, for example, linear, olive, wheel, helical, cubane, rectangular, chair and boat conformations, have been successfully obtained.[4–7] On the other hand, the design and construction of metal–organic polymers have attracted great interest in recent years, owing to their variety of structures, interesting properties and potential applications in the fields of catalysis, luminescence, gas adsorption, and magnetic materials.[8–10] In both cases, the structures of molecular clusters and coordination polymers are dependent upon the chemical structures of the ligand, metal ions, anions, pH value, metal-to-ligand ratio and solvents.[11–16] The most important factor among these that controls molecular structures is ligands with suitably disposed bridging groups. Generally, ligands appended with potentially endogenous bridging groups linking metal ions in a closed-cluster system (*e.g.* cubane, rectangular, chair, boat cluster) have been widely used for the design and synthesis of coordination clusters.[17] On the other hand, pyridine base ligands containing amide groups generally are coordinated to the metal centers through their pyridyl nitrogen atoms and interact with each other *via* hydrogen bonds involving the amide groups, which are important for molecular recognition and constructing supramolecular arrays.[18] However, there is still a very long way to go to develop new architectures of coordination polymers using specific spacer ligands in order to rationalize the design of compounds with well-defined

[a] *Department of Inorganic Chemistry, Faculty of Chemistry, University of Tabriz, P.O. Box 5166616471, Tabriz, Iran. E-mail: akhandar@yahoo.com*
[b] *Department of Chemistry, Faculty of Science, University of Maragheh, P.O. Box 55181-83111, Maragheh, Iran. E-mail: mahmoudi_ghodrat@yahoo.co.uk*
[c] *Institute of General and Ecological Chemistry, Faculty of Chemistry, Lodz University of Technology, Żeromskiego 116, 90-924 Łódź, Poland*
[d] *Department of Chemistry, Baku State University, Z. Khalilov str. 23, AZ 1148, Baku, Azerbaijan*
[e] *Organic Chemistry Department, RUDN University, 6 Miklukho-Maklaya str., Moscow 117198, Russian Federation*
[f] *Sinop University, Scientific and Technological Research Application and Research Center, 57000 Sinop, Turkey*
[g] *Department of Chemistry, Faculty of Arts and Sciences, Eskişehir Osmangazi University, 26480 Eskişehir, Turkey*
[h] *Departamento de Quimica, Universitat de les Illes Balears, Crta. de Valldemossa km 7.5, 07122 Palma de Mallorca (Baleares), Spain. E-mail: toni.frontera@uib.es*
† Electronic supplementary information (ESI) available: Tables S1–S3 and Hirshfeld analysis of the complexes. CCDC numbers 1524914–1524920. For ESI and crystallographic data in CIF or other electronic format see DOI: 10.1039/c6ce02666d

structures and useful functions. The ability to predict and control the structure and topology of coordination clusters and polymers remains an elusive goal, and much more work is required to understand the inter- and intra-molecular forces that determine the patterns of molecular structure and crystal packing.

In this work, we chose two pyridine base ligands, HL^1 and HL^2 (Scheme 1), as chelating-bridging ligands whose main difference is the position of pyridinic nitrogen, and this slight difference leads to interestingly big differences on the structures of the products. Ligand flexibility, combined with the donor-rich nature of this type of ligand, leads to a situation where, in addition to rotational variations, different structural motifs occur through various combinations of the diazine and other donor groups. Ligands such as HL^2 (Scheme 1) have $O_{(C=O)}$ and/or $N_{(py)}$ groups adjacent to the diazine. This rich coordination ability gives the possibility to generate, through self-assembly reactions with M(II) salts, polynuclear clusters with four and five metals.[19] On the other hand, ligands such as HL^1 have great bridging-chelating ability that is adequate for the design and construction of metal–organic coordination polymers because of the *para* position of the pyridinic nitrogen.[19]

In this manuscript, we report on the systematic syntheses and structural characterization of Zn(II) and Cd(II) complexes of a series of unsymmetrical Schiff base ligands. The aim of this study is to analyse the competition between anions and ligands HL^n (Scheme 1) for the coordination sites at the metal(II) centre and to probe how the nature of the anion affects the crystal packing. The structural descriptions have been corroborated with calculations of Hirshfeld surfaces, which reveal a strong effect of noncovalent interactions on the properties of the surfaces. Finally, the interesting conventional and unconventional π–π stacking interactions observed in the solid state of some compounds have been analysed both energetically and using Bader's theory of atoms in molecules by means of DFT calculations.

Experimental and theoretical methods

Experimental

Materials and measurements. All the reagents were commercially available and employed without further purification. Microanalyses were carried out using a Heraeus CHN-O-Rapid Analyser. FT-IR spectra were recorded on a Bruker Tensor 27 FT-IR spectrometer with KBr disks in the range 4000–400 cm^{-1}. Single crystals suitable for X-ray analyses were used for intensity data collection on a Bruker AXS SMART APEX CCD diffractometer using graphite monochromated MoKα radiation (λ = 0.71073 Å) at different temperatures (Table S1†).

The hydrazone ligands HL^1 and HL^2 were prepared according to the literature.[20,21]

Synthesis of $Zn(HL^1)Br_2$ (1), $Zn(HL^1)Cl_2$ (2) and $[Cd(HL^1)_2](NO_3)_2{\cdot}H_2O$ (3). A solution of the ligand HL^1 (0.151 g, 0.5 mmol) in 30 ml of methanol was treated with a methanolic solution of the appropriate zinc(II)/cadmium(II) salt (0.5 mmol). The solution was heated under reflux for 3 h. The resulting solution was allowed to stand at room temperature, and after slow evaporation, crystals separated out, which were collected, washed with ether and dried over P_4O_{10} *in vacuo*.

$Zn(HL^1)Br_2$ (1). Yield: 57% (0.184g). Anal. calc. for $C_{12}H_{10}Br_2N_4OZn$: C, 31.93; H, 2.23; N, 12.41. Found: C, 32.08; H, 2.44; N, 12.32%. IR (KBr cm^{-1}) selected bands: 3156, 2928, 1650, 1530, 1468, 1441, 1351, 1294, 1218, 1158, 1091, 932, 869, 779, 751, 665.

$Zn(HL^1)Cl_2$ (2). Yield: 59% (0.107g). Anal. calc. for $C_{12}H_{10}Cl_2N_4OZn$: C, 39.76; H, 2.78; N, 15.46. Found: C, 39.91; H, 2.86; N, 15.31%. IR (KBr cm^{-1}) selected bands: 3190, 2927, 1645, 1534, 1467, 1441, 1349, 1296, 1215, 1156, 1091, 936, 844, 780, 750, 665.

$[Cd(HL^1)_2](NO_3)_2{\cdot}H_2O$ (3). Yield: 59% (0.114 g). Anal. calc. for $C_{24}H_{22}N_{10}O_9Cd$: C, 40.78; H, 3.14; N, 15.90. Found: C, 40.59; H, 3.51; N, 15.66%. IR (KBr cm^{-1}) selected bands: 3449, 3421, 3180, 3100, 1661, 1550, 1458, 1386, 1221, 1124, 1063, 1041, 1019, 840, 754, 709.

Synthesis of $Cd(HL^2)Br_2$(4), $Zn(HL^2)Cl_2$ (5) and $Zn(HL^2)Br_2$ (6). Compounds **4–6** were prepared using the ligand HL^2 (0.113 g, 0.5 mmol) instead of HL^1 by the same method as for compounds **1–3**.

$Cd(HL^2)Br_2$(4). Yield: 64% (0.184g). Calc. for $C_{18}H_{14}Br_2CdN_4O$: C, 37.63; H, 2.46; N, 9.75. Found: C, 37.47; H, 2.45; N, 9.60%. IR (KBr cm^{-1}) selected bands: 3277, 3053, 1583, 1492, 1460, 1428, 1325, 1274, 1194, 1132, 1089, 910, 784, 743, 704.

$Zn(HL^2)Cl_2$ (5). Yield: 64% (0.130g). Calc. for $C_{18}H_{14}Cl_2N_4OZn$: C, 49.29; H, 3.22; N, 12.77. Found: C, 49.44; H, 2.97; N, 12.59%. IR (KBr cm^{-1}) selected bands: 3296, 3065, 1661, 1587, 1461, 1432, 1331, 1274, 1238, 1140, 1094, 913, 788, 747, 705.

$Zn(HL^2)Br_2$ (6). Yield: 59% (0.156g). Calc. for $C_{18}H_{14}Br_2N_4OZn$: C, 40.98; H, 2.68; N, 10.62. Found: C, 40.83; H, 2.73; N, 10.43%. IR (KBr cm^{-1}) selected bands: 3202, 1652, 1509, 1469, 1371, 1223, 1164, 1053, 909, 842, 749, 685.

Synthesis of $\{[Zn_4(L^2)_4I_2][ZnI_4]{\cdot}2H_2O\}$ (7). A solution of the ligand HL^2 (0.151 g, 0.5 mmol) in methanol was treated with a methanolic solution of $Zn(OAc)_2$ $2H_2O$ (0.109 g, 0.5 mmol). The solution was heated under reflux, and sodium iodide

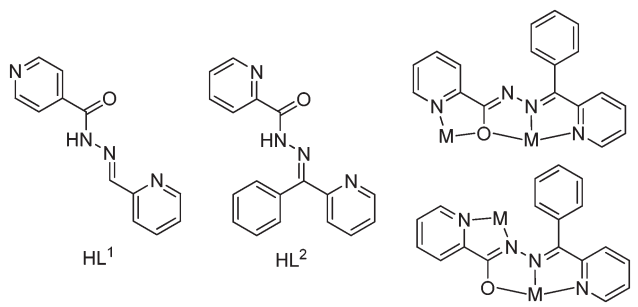

Scheme 1 The structures of the ligands used herein and the coordination modes of (L^2).

(0.149 g, 1 mmol) was added in portions to the solution and then further refluxed for 3 h. The resulting solution was allowed to stand at room temperature, and upon slow evaporation, gave crystals. The crystals that separated out were collected, washed with ether and dried over P_4O_{10} *in vacuo*. Yield: 59% (0.156g). Calc. for $C_{72}H_{52}I_6N_{16}O_8Zn_5$: C, 36.68; H, 2.22; N, 9.51. Found: C, 36.78; H, 2.13; N, 9.63%. IR (KBr cm^{-1}) selected bands: 3202, 1570, 1520, 1470, 1366, 1207, 1163, 1052, 974, 790, 753, 652.

X-ray crystallography

Suitable crystals of **1**–**7** (see Scheme 2) were selected for data collection which was performed using Bruker APEX-II, STOE IPDS and Supernova diffractometers equipped with graphite monochromatic Mo-K_α radiation. The structures were solved by direct methods using SHELXS-97 (ref. 22) and refined by the full-matrix least-squares methods on F^2 using SHELXL-97 (ref. 22) from within the WINGX (ref. 23) suite of software. All non-hydrogen atoms were refined with anisotropic parameters. The H atoms were located from different maps and then treated as riding atoms with C–H distances of 0.93 Å and N–H distances of 0.86 Å. For compounds **6** and **7** of triclinic cells, the STOE IPDS-1 equipment did not allow us to collect over 91–92% fraction of the reflections. However, the structural characterization of these compounds (with a final *R* factor of *ca.* 3%) is conclusive as to the general shape of the complexes. A suitable absorption correction was applied to all data sets. Molecular diagrams were created using MERCURY.[24] Supramolecular analyses were conducted and the diagrams were prepared with the aid of PLATON.[25] The details of the crystal parameters, data collection and refinements are summarized in Table S1.† The selected lengths and angles are listed in Table S2.†

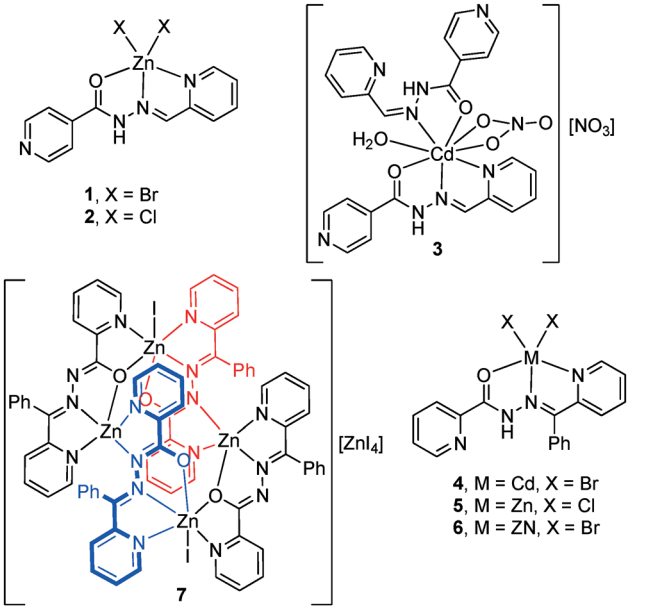

Scheme 2 Complexes **1**–**7** reported herein.

Hirshfeld surface analysis. The Hirshfeld (HF) surfaces[26] and the related 2D-fingerprint plots[27] were calculated using Crystal Explorer.[28] The CIF file of each structure was imported into Crystal Explorer and high resolution Hirshfeld surfaces were mapped with the function d_{norm}. Before starting the calculations, the bond lengths to hydrogen atoms were set to standardized neutron values (O–H = 0.983Å, N–H = 1.009Å and C–H = 1.083Å). Then, the HF surfaces were resolved into 2D-fingerprint plots, in order to quantitatively determine the nature and type of all intermolecular contacts experienced by the molecules in the crystal.

Computational methods

The geometries of the complexes included in this study were computed at the wB97XD/6-31+G* level of theory using the crystallographic coordinates within the Gaussian-09 program.[29] This level of theory which includes the dispersion correction (D) is adequate for studying noncovalent interactions dominated by dispersion effects like π-stacking.[30] We have used the crystallographic coordinates instead of optimized complexes because we are interested in estimating the binding energies of several assemblies as they stand in the crystal structure, instead of investigating the most favourable geometry for a given complex. The "atoms-in-molecules" (AIM) analysis of the electron density has been performed at the same level of theory using the AIMAll program.[31]

Results and discussion

Crystal structures $[Zn(HL^1)X_2]$ (1–2)

Compounds **1** and **2** crystallize in the $P2_1/c$ space group, in which the zinc cation is neutralized by two Br^- and Cl^- anions, respectively. The compounds are composed of the mononuclear unit, $[Zn(HL^1)X_2]$ X = Br^- (**1**) and Cl^- (**2**), in which the ligand adopts an extended conformation with the aryl ring in the *trans* position with respect to the imine moiety (see Fig. 1). The linker coordinates the Zn(II) through three coplanar ligating sites involving the carbonyl O, the hydrazine N and the pyridyl nitrogen, with bond distances shown in Table 1, generating two five-membered chelate rings. Moreover, two X^- anions are located in essentially apical positions, above and below, the mean plane defined by the donating centers of the ligand resulting in a distorted tetragonal pyramidal geometry.

In both compounds, the N–H groups are involved in intermolecular hydrogen bonds to the bromide/chloride atoms with distances of 3.385(4)/3.472(4) for **1** and 3.225(3)/3.318(3) Å for **2** (see Fig. 2). These H-bonds facilitate the formation of infinite 1D columns with an antiparallel arrangement of the mononuclear complexes. These supramolecular 1D columns are further stabilized by stacking π–π interactions between the coordinated and uncoordinated pyridyl rings with centroid-to-centroid distances ranging from 3.68 to 3.96 Å

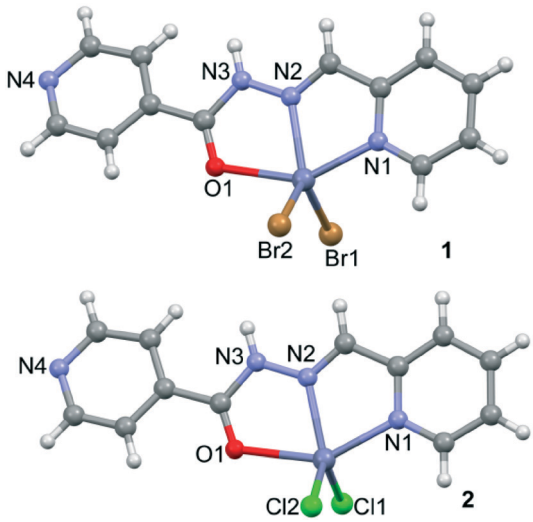

Fig. 1 X-ray structures of isostructural complexes **1** and **2** and the atomic numbering scheme.

Table 1 Bond distances (Å) in the coordination environment for **1** and **2**

Cmpnd	1	2
Zn1–O1	2.319(3)	2.308(3)
Zn1–N1	2.145(4)	2.153(3)
Zn1–N2	2.117(4)	2.122(3)
Zn–X$^-$	2.3715(8), 2.3605(8)	2.253(1), 2.233(1)

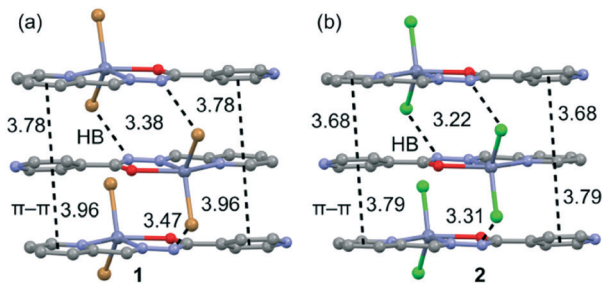

Fig. 2 Stacking interactions present in **1** (a) and **2** (b). Distances are in Å.

(see Fig. 2). The atoms belonging to the chelate ring also participate in this stacking interaction, which is further discussed below in the theoretical study. Finally, the crystal structures are also stabilized by weak C–H···X (X = Cl, Br) and C–H···O noncovalent interactions.

Crystal structure of $[Cd(HL^1)_2](NO_3)_2{\cdot}H_2O$ (3)

The molecular structure of **3** with atom labelling is shown in Fig. 3. The asymmetric unit of **3** contains one Cd(II) ion, two HL^1 ligands, one coordinated nitrate anion, one coordinated aqua ligand and one non-coordinated nitrate anion. The

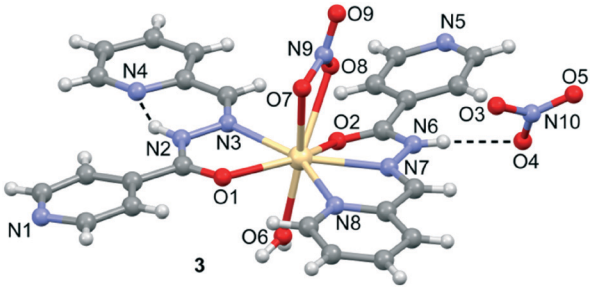

Fig. 3 Perspective view of Cd-complex **3** and the atomic numbering scheme.

Cd(II) ion is coordinated by three nitrogen atoms and two oxygen atoms from two different HL^1 ligands, two oxygen atoms from the nitrate anion and one oxygen atom from the aqua ligand. Therefore, the coordination mode of each ligand is different. That is, one ligand is *N*,*N*,*O*-tridentate, as observed in the mononuclear Zn(II) complexes **1** and **2**. However, the other ligand is only *N*,*O*-bidentate and, curiously, adopts a *cis* conformation, thus facilitating the formation of an intramolecular N–H···N hydrogen bonding interaction (see Fig. 3). The Cd–N bond distances (see Table S2†) range between 2.358(3)–2.412(3) Å, both Cd–$O_{carboxyl}$ bond distances are 2.398(2) and 2.547(2) Å, and the Cd–$O_{nitrate}$ bond distances are 2.454(3) and 2.570(3) Å. The non-coordinated nitrate anion establishes a hydrogen bonding interaction with the acidic N6–H group.

Crystal structures of $Cd(HL^2)Br_2$ (4), $Zn(HL^2)Cl_2$ (5) and $Zn(HL^2)Br_2$ (6)

Isostructural compounds **4** (M = Cd, X = Br), **5** (M = Zn, X = Cl) and **6** (M = Zn, X = Br) crystallize in the $P\bar{1}$ space group, in which M(II) (M = Cd, Zn) is neutralized by two Cl^- or two Br^- anions. The asymmetric unit of **4**–**6** is composed of two mononuclear Zn complexes (see Fig. 4 for an illustration of complex **4**). The ligand coordinates the Cd(II) atom through three coplanar ligating sites involving the carbonyl O, the hydrazine N and the pyridyl nitrogen forming two five-membered chelate rings. The main difference between the mononuclear complexes A and B present in the asymmetric unit is the dihedral angle between the imino group and the

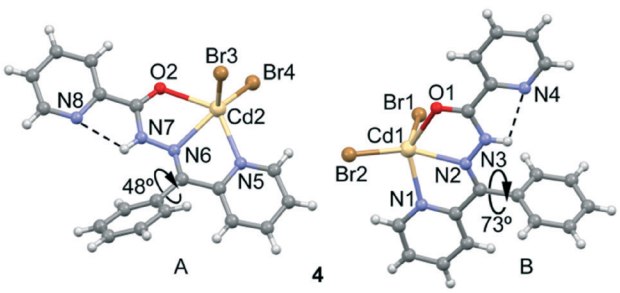

Fig. 4 Perspective view of the two similar mononuclear Cd complexes present in **4**.

phenyl group bonded to C6. The dihedral angles have values of 48.5° and 73.4° for **4**, 52.2° and 85.7° for **5**, and 49.0° and 82.6° for **6**. Moreover, the halides are located in essentially apical positions, above and below, the mean plane defined by the donating centers. The M–O bond distances (see Table S2†) are, for units A and B, 2.437(2) and 2.461(2) Å in **4**, 2.326(1) and 2.4010(16) Å in **5**, and 2.325(2) and 2.412(2) Å in **6**, respectively. The M–N bond distances ranged between 2.334(2)–2.371(2) Å in **4**, 2.124(2)–2.141(2) Å in **5**, and 2.121(2)–2.153(2) Å in **6**, while the M–R (R = Br in **4**, Cl in **5** and Br in **6**) bond distances ranged between 2.5035(5)–2.5547(4) Å in **4**, 2.1926(5)–2.2410(7) Å in **5**, and 2.3374(5)–2.3803(5) Å in **6**.

Finally, the crystal packing of both compounds presents self-assembled dimers governed by chelate ring···chelate ring interactions (see Fig. 5). These dimers are only formed between the units of the crystal with a larger dihedral angle (see Fig. 4, right), which is likely due to the almost orthogonal arrangement of the phenyl ring with respect to the chelate ring. This facilitates the antiparallel approximation of the chelate rings (centroid-to-centroid distances are 3.45 Å in **4**, 3.50 Å in **5** and 3.49 Å in **6**). This chelate ring···chelate ring interaction is further studied below. This type of self-assembled dimers has been recently studied in Hg(II) complexes with the same ligand.[21b] The crystal structures are further stabilized by weak C–H···X and C–H···O noncovalent interactions.

Crystal structures of $[Zn_4(L^2)_4I_2][ZnI_4].2H_2O$

Compound **7** (Fig. 6) crystallizes with $Z' = 1/2$ in the space group $C2/c$. The asymmetric unit of **7** contains three Zn(II) ions, two L^2 ligands, three I anions and two non-coordinated water molecules. The structure of **7** includes a cationic tetranuclear cluster of four Zn(II) ions, four L^2 ligands, and two I anions, counterbalanced by a ZnI_4^{2-} ion. The Zn···Zn separations are 4.132 Å and 5.019 Å. The L^2 ligand self-assembles in the presence of Zn(II) to give a rectangular [2 + 2] grid complex (Fig. 7), with two ligands bridging adjacent Zn(II) ions on the short sides of the rectangle with an alkoxide oxygen, and two bridging the adjacent Zn(II) ions on the long sides of the rectangle with N–N diazine groups. In **7**, the Zn(II) ions are of three coordination types. Firstly, the Zn1 atom is coordinated

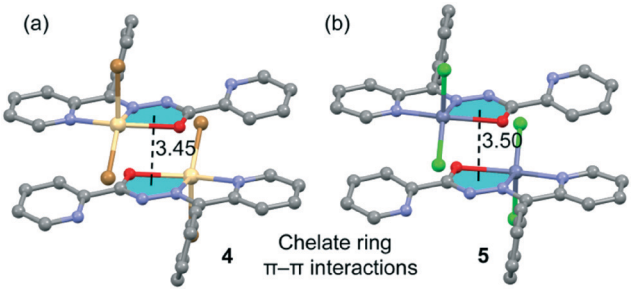

Fig. 5 Self-assembled stacked dimers present in **5** (a) and **6** (b). Distances are in Å. H-atoms are omitted for clarity.

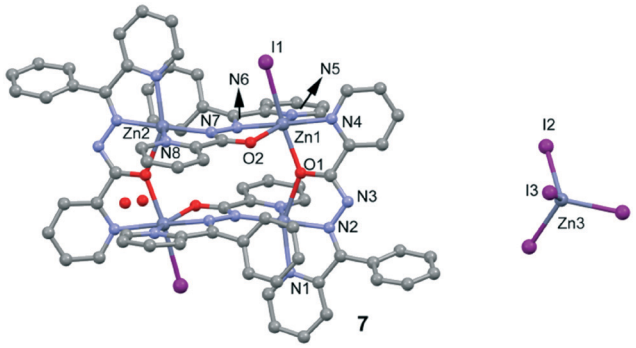

Fig. 6 Perspective view of complex **7** and the atom numbering scheme. H-atoms are omitted for clarity.

by three nitrogen atoms and two oxygen atoms from two different L^2 ligands and one coordinated I atom, thus showing an octahedral coordination geometry. Secondly, the Zn2 atom is coordinated by four nitrogen atoms and one oxygen atom from two different L^2 ligands, thus showing a square pyramidal coordination geometry. Finally, the Zn3 atom is located on a symmetry center and is coordinated by four I atoms, thus showing a tetrahedral coordination geometry. The bond distances of Zn–N (see Table S2†) ranged between 2.044(5)–2.174(6) Å and the other Zn–O bond lengths ranged between 2.121(5)–2.235(4) Å, respectively.

It should be mentioned that the isolation of a tetrahedral tetraiodozincate anion in the solid state of **7** is quite surprising since its stability is the lowest of the tetrahalozincate ZnX_4^{2-} series (X = Cl, Br, I). Therefore, formation of such a complex in the case of iodide, but not chloride or bromide (complexes **5** and **6**) is rather unexpected. We do not have a convincing explanation for this experimental finding, although the different behaviour of **7** with respect to **5** and **6** could be related to the different protonation state of the ligand. The different behaviour of a series of tetrahalometallate anions MX_4^{2-} (M = Zn, Cd and Hg; X = Cl, Br and I) determining the solid state architecture of

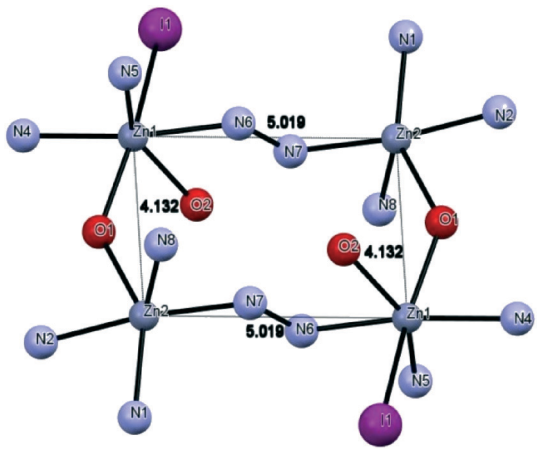

Fig. 7 Tetranuclear rectangular [2 + 2] complex of **7**.

different 2-phenylethylammonium salts has been analysed.[32] Moreover, the different behaviour of tetraiodozincate with respect to Cl and Br analogues in the synthesis of hybrid metal–organic salts has also been reported.[33] Although the isolation of tetraiodozincate is not very common, several works have appeared in the literature, including tetrahedral ZnI_4^{2-} solid state X-ray structures, in the past decade.[34]

Hirshfeld surface analysis

The intermolecular interactions in crystal structures **1**–**7** were quantified using Hirshfeld surface analysis and fingerprint plots (FP). The dominant intermolecular interactions are viewed as a bright red area on the d_{norm} surface. Fig. 8 illustrates samples of Hirshfeld surfaces for structures **3** and **7**. In general, the Hirshfeld surface analysis suggests that the crystal packing in structures **1**–**7** is largely dominated by the common planar components of ligands, leading to close H···H intercontacts as well as interesting C–H···π and π···π stacking interactions. In **3**, we observe a high level of O···H interactions due to the hydrogen bonds between solvents molecules and the complex. The Cl···H, Br···H and I···H H-bonding interactions are also very important.

The two-dimensional fingerprint plots of the HS for structures **1**–**7** are shown in Fig. S1 (ESI†). The quantitative comparison of the intercontacts for all structures and the relevant intermolecular interactions are presented in Table S3 (ESI†). From this analysis, the division of contributions is possible for different interactions, including H···H, O···H, C···H, C···C, N···C, N···H, O···N, N···N (for all compounds), Cl···H, Cl···C [in **2** and **5**], Br···H, Br···C [in **1**, **4** and **6**] and I···H and I···C [in **7**], which commonly overlap in the full fingerprint plots. The fingerprint plots of compounds **1**–**7** show that the dominant interactions are H···H (22.5–41.1%) and C···H (7.2–20.4%). The C···H contacts represent the C–H···π interactions in the crystals, and the highest values were measured in **4**, **5** and **6**. For π–π interactions which correspond to the C···C contacts, the highest values were measured in **1**, **2** and **3**. The O···H and X···H hydrogen bonding (where X = Cl, Br, I) also play very important roles in stabilizing the structures. The O···H interactions vary from 5.1–5.3% for **4**, **5** and **6** to 31.7% for **3**, while the X···H contacts vary from 17.9 % for **7** to 35.9% for **1**.

Theoretical Study

We have focused the theoretical study on the comparison of the energetic features of the different types of π-stacking interactions (chelate ring–π and π–π) observed in the crystal packing of compounds **1**–**2** and **4**–**6** described above (see Fig. 2 and 5). In particular, we have analysed the π–π and chelate ring···chelate ring stacking interactions which are crucial to understanding the crystal packing of complexes **1**–**7**, as discussed above. Predictable π-stacking[35] interactions involve organic aromatic molecules; however, other planar molecular fragments can also participate in more "unpredictable" stacking interactions.[36] Among them, chelate rings with delocalized π bonds establish stacking[36] interactions similar to those of aromatic organic molecules[35i–l] in transition metal complexes. The existence of chelate-ring–π interactions is associated with the aromaticity of planar chelate rings with delocalized π bonds.[37]

First of all, in order to study the donor–acceptor ability of the $ZnHL^1X_2$ and MHL^2X_2 (M = Cd, Zn) complexes, we have computed the molecular electrostatic potential (MEP) surface of a model system (compound **2**), which is shown in Fig. 9. As expected, the most negative electrostatic potential corresponds to the region of the Cl ligands while the most positive part is located in the region of the N,C–H groups at the molecular plane. Therefore, H-bonding interaction between these groups (N–H···X) should be electrostatically favoured.

Furthermore, perpendicularly to the molecular plane, we found that each 5-membered chelate ring has almost negligible MEP values (−5 kcal mol^{-1}). The MEP values are positive over the pyridine rings due to the effect of the coordination to the Zn. Therefore, pyridine–pyridine interactions (conventional π-stacking) should be electrostatically less favoured (electrostatic repulsion) than chelate ring···chelate ring interactions.

In isostructural compounds **1**–**2**, we have computed the interaction energy of the self-assembled π-stacked dimers shown in Fig. 10a which are responsible for the formation of the 1D columns shown in Fig. 2. The self-assembled dimers are stabilized by a combination of H-bonds and π–π stacking interactions, including the C═N–N–C(O) part of the ligand. The dimerization energies in **1** and **2** (ΔE_1 = −58.7 kcal mol^{-1}

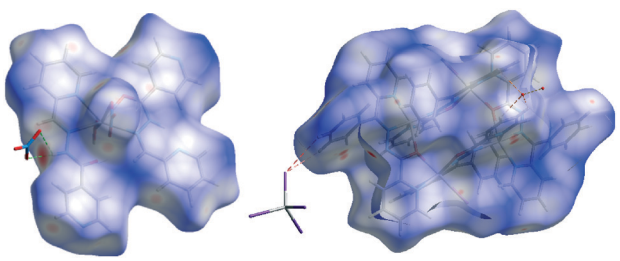

Fig. 8 Views of the Hirshfeld surfaces for **3** (left) and **7** (right) mapped with d_{norm}.

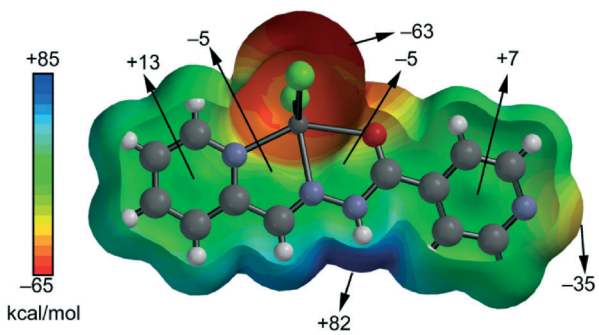

Fig. 9 MEP surface of compound **2**. The MEP values at selected points are given in kcal mol^{-1}.

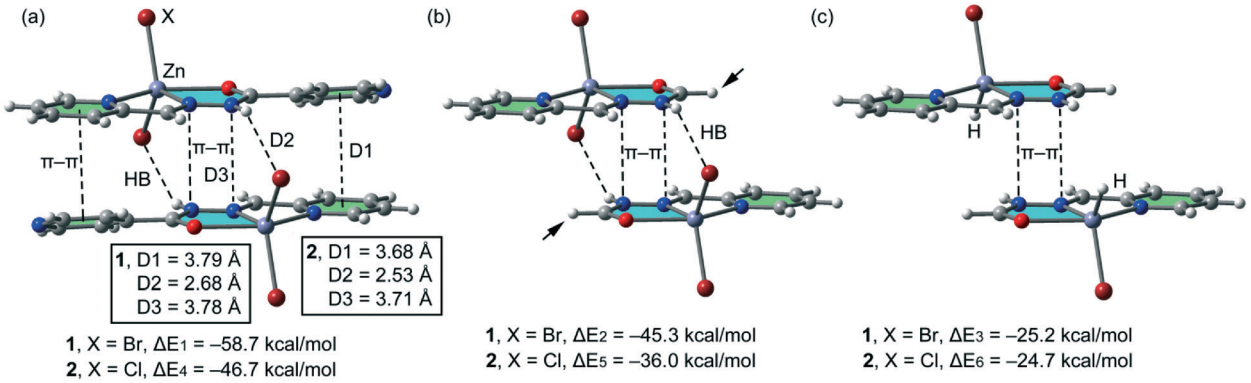

Fig. 10 (a) Interaction energies of the self-assembled π-stacked dimers observed in the solid state of compounds **1**–**2**. (b and c) Interaction energies in several theoretical models of **1** and **2**.

and ΔE_4 = −46.7 kcal mol^{-1}, respectively) are very large due to the contribution of both H-bonding and π–π interactions, the latter involving a very extended π-system and the former encompassing the most positive part of the complex (N–H group) and the most negative (belts of the halido ligands). In an effort to calculate the contribution of the different forces that govern the formation of the self-assembled dimers, we have computed a theoretical model where the uncoordinated pyridine rings have been replaced by H atoms (see the small arrows in Fig. 10b) and consequently, the π–π stacking interactions between the coordinated and uncoordinated pyridine rings are not formed. As a result, the interaction energies are reduced to ΔE_2 = −45.3 kcal mol^{-1} and ΔE_5 = −36.0 kcal mol^{-1} in **1** and **2**, respectively. Therefore, the contribution of both symmetrically equivalent π–π stacking interactions can be roughly estimated by difference (they are −13.4 and 10.7 kcal mol^{-1} for **1** and **2**, respectively). Furthermore, we have used an additional dimer, where the halido ligand that participates in the H-bonding interactions has been replaced by hydride, and consequently, the H-bonding interactions are not formed. The resulting interaction energies are further reduced to ΔE_3 = −25.2 kcal mol^{-1} and ΔE_6 = −24.7 kcal mol^{-1} for **1** and **2**, respectively, which corresponds to the contribution of the π–π stacking interactions between the C=N–N–C(O) part and other long range van der Waals interactions. The contribution of both H-bonding interactions can be estimated by difference (they are −20.1 and −11.3 kcal mol^{-1} for **1** and **2**, respectively). Therefore, the H-bonding interactions are stronger in compound **1**, which is likely due to the larger polarizability of Br^- with respect to Cl^-.

In the isostructural compounds **4**–**6**, the π-stacking binding mode is different to the one observed for **1** and **2**. As previously mentioned, a chelate ring···chelate ring π–π interaction is formed, in addition to the H-bonding and conventional π–π interactions (see Fig. 11a). We have studied theoretically the energetic features of the dimers of compounds **4** (Cd) and **6** (Zn) to analyse the effect of the metal center. Interestingly, the chelate ring···chelate ring distance is significantly shorter (3.44 Å for **4** and 3.50 Å for **5** and **6**) than the distance of the π–π stacking interaction between the C=N–N–C(O) moieties in **1** and **2** (see Fig. 10a). Moreover, the H-bonding distances are longer in compounds **4** and **6** with respect to compounds **1** and **2**. As a consequence, the computed interaction energies of the self-assembled dimers **4** and **6** (ΔE_7 = −52.7 kcal mol^{-1} and ΔE_{10} = −53.9 kcal mol^{-1}, respectively) are similar to those computed for **1** and **2** due to a

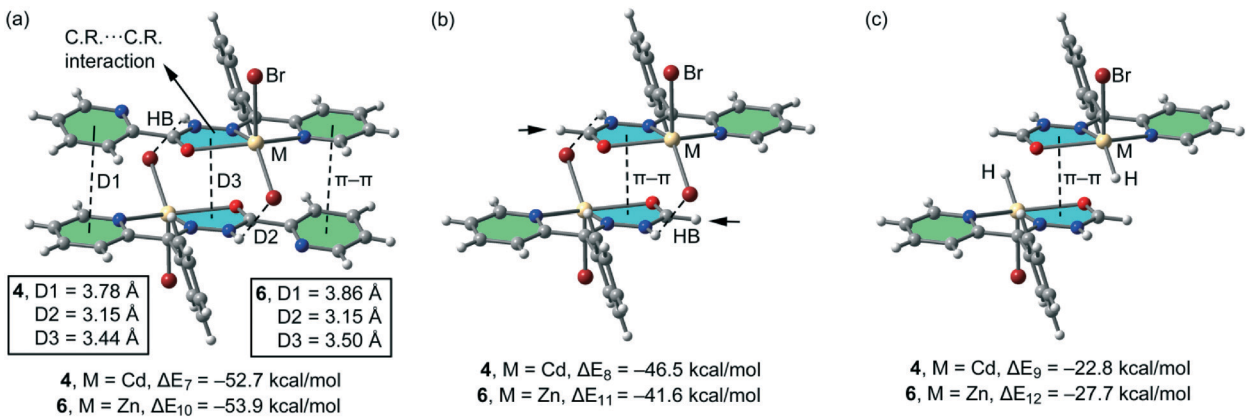

Fig. 11 (a) Interaction energies of the self-assembled π-stacked dimers observed in the solid state of compounds **4** and **6**. (b and c) Interaction energies in several theoretical models of **4** and **6**.

compensating effect between the longer H bond and the shorter chelate ring···chelate ring interaction. In an effort to calculate the contribution of the different interactions, we have computed a theoretical model where the uncoordinated pyridine rings have been replaced by H atoms (see the small arrows in Fig. 11b) and consequently the conventional π–π stacking interactions are not formed. As a result, the interaction energies are reduced to ΔE_8 = −46.5 kcal mol^{-1} and ΔE_{11} = −41.6 kcal mol^{-1} in **4** and **6**, respectively. Therefore, this contribution (both π–π interactions) can be roughly estimated by difference (−6.2 and −12.3 kcal mol^{-1} for **4** and **6**, respectively). These values are likely underestimated because the substitution of the uncoordinated pyridine by a H-atom reinforces the N–H···X H-bonding due to the elimination of the intramolecular N–H···N(Py) H-bond. Furthermore, we have used an additional dimer, where the halido ligands that participate in the H-bonding interactions have been replaced by hydride, and consequently, the H-bonding interactions are not formed. The interaction energies are further reduced to ΔE_9 = −22.8 kcal mol^{-1} and ΔE_6 = −27.7 kcal mol^{-1} for **4** and **6**, respectively, which corresponds to the contribution of the chelate ring···chelate ring π–π stacking interactions and other long range van der Waals interactions.

In order to provide additional evidence of the existence of unconventional π–π stacking interactions between the C═N–N–C(O) moieties and the chelate-ring interactions, we have analysed the self-assembled π-stacked dimers of compounds **2** and **5** (as exemplifying models) using Bader's theory of "atoms in molecules" (AIM),[38] which provides an unambiguous definition of chemical bonding. The AIM theory has been successfully used to characterize and understand a great variety of interactions including those described herein.[39] In Fig. 12, we show the AIM analysis of compounds **2** and **5**. In **2**, it can be observed that each conventional π–π interaction (pyridine rings) is characterized by the presence of one bond critical point that interconnects two carbon atoms of the coordinated and uncoordinated pyridine rings, thus confirming the interaction. Furthermore, the distribution of critical points reveals the existence of two symmetrically related N–H···Cl H-bonding interactions. Each one is characterized by a bond critical point and a bond path connecting one H atom of the NH group with the Cl ligand. Finally, the unconventional π–π interactions between the C═N–N–C(O) moieties is confirmed by the presence of four bond critical points interconnecting the C═N–N–C(O) groups. In **5**, the π–π interaction (pyridine rings) is characterized by the presence of two bond critical points and bond paths that connect two carbon atoms of the coordinated pyridine to two carbon atoms of the uncoordinated one. Furthermore, the distribution of critical points reveals the existence of two types of H-bonding interactions: N–H···Cl and C–H···O (chelate ring). This ancillary C–H···O interaction explains the large interaction energy obtained for the chelate ring···chelate ring π–π interaction (see Fig. 11c). Finally, the chelate ring···chelate ring interaction is characterized by two bond critical points and bond paths that connect the O atom of one ring to the nitrogen atom of the other chelate ring and *vice versa*, thus validating the existence of the interaction. The value of the Laplacian of the charge density at the bond critical points is positive, as is common in closed-shell interactions.

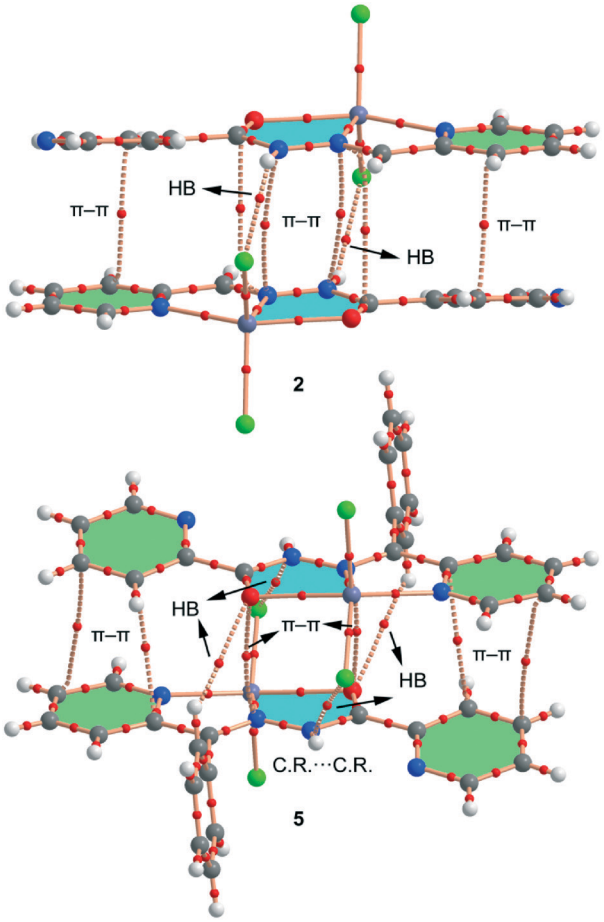

Fig. 12 AIM analysis of the self-assembled dimers retrieved from the X-ray structures of compounds **2** and **5**. Only bond critical points are represented by red spheres. The bond paths connecting the bond critical points are also represented by dashed lines.

Concluding remarks

We reported the syntheses and X-ray structural characterization of seven new metal complexes of Cd(II) and Zn(II) metal centers with two hydrazine-based ligands. Most compounds exhibit remarkable chelate ring–chelate ring and π–π stacking interactions in the solid state that have been studied using DFT calculations and Hirshfeld analysis. These interactions are crucial for the formation of supramolecular self-assembled dimers in the solid state. The energies associated with the interactions, including the contribution of the different forces, have been evaluated. In general, the chelate–chelate interactions are stronger than those those reported for conventional π–π complexes,[40] which is attributed to the co-existence of other long range van der Waals interactions. The results reported herein might be useful to understand the

solid state architecture of MOF materials that contain M(II)-chelate rings and organic aromatic molecules.

Acknowledgements

We are grateful to the University of Tabriz Research Council for the financial support of this research. This work was supported by the Ministry of Education and Science of the Russian Federation (Agreement number 02.a03.21.0008). A. F. thanks the DGICYT of Spain (project CTQ2014-57393-C2-1-P, FEDER funds). We thank the CTI (UIB) for the computational facilities.

Notes and references

1 (*a*) K. C. Mondal, A. Sundt, Y. H. Lan, G. E. Kostakis, O. Waldmann, L. Ungur, L. F. Chibotaru, C. E. Anson and A. K. Powell, *Angew. Chem., Int. Ed.*, 2012, **51**, 7550–7554; (*b*) C. M. Liu, R. G. Xiong, D. Q. Zhang and D. B. Zhu, *J. Am. Chem. Soc.*, 2010, **132**, 4044–4045; (*c*) H. Q. Tian, L. Zhao, Y. N. Guo, Y. Guo, J. K. Tang and Z. L. Liu, *Chem. Commun.*, 2012, **48**, 708–710.

2 (*a*) H. X. Li, W. Zhao, H. Y. Li, Z. L. Xu, W. X. Wang and J. P. Lang, *Chem. Commun.*, 2013, **49**, 4259–4261; (*b*) R. M. Haak, A. Decortes, E. C. Escudero-Adan, M. M. Belmonte, E. Martin, J. Benet-Buchholz and A. W. Kleij, *Inorg. Chem.*, 2011, **50**, 7934–7936.

3 (*a*) L. Q. Mo, J. H. Jia, L. J. Sun and Q. M. Wang, *Chem. Commun.*, 2012, **48**, 8691–8693; (*b*) K. F. Konidaris, V. Bekiari, E. Katsoulakou, C. P. Raptopoulou, V. Psycharis, E. Manessi-Zoupa, G. E. Kostakis and S. P. Perlepes, *Dalton Trans.*, 2012, **41**, 3797–3806.

4 (*a*) I. W. P. Chen, M. D. Fu, W. H. Tseng, J. Y. Yu, S. H. Wu, C. J. Ku, C. H. Chen and S. M. Peng, *Angew. Chem., Int. Ed.*, 2006, **45**, 5814–5818; (*b*) S. K. Kondaveeti, S. Vaddypally, C. Lam, D. Hirai, N. Ni, R. J. Cava and M. J. Zdilla, *Inorg. Chem.*, 2012, **51**, 10095–10104.

5 X. L. Tang, W. H. Wang, W. Dou, J. Jiang, W. S. Liu, W. W. Qin, G. L. Zhang, H. R. Zhang, K. B. Yu and L. M. Zheng, *Angew. Chem., Int. Ed.*, 2009, **48**, 3499–3502.

6 (*a*) N. Hoshino, A. M. Ako, A. K. Powell and H. Oshio, *Inorg. Chem.*, 2009, **48**, 3396–3407; (*b*) H. Oshio, N. Hoshino, T. Ito, M. Nakano, F. Renz and P. Gutlich, *Angew. Chem.*, 2003, **115**, 233–235.

7 Y. Y. Pang, S. X. Cui, B. Li, J. P. Zhang, Y. Wang and H. Zhang, *Inorg. Chem.*, 2008, **47**, 10317–10324.

8 (*a*) A. R. Millward and O. M. Yaghi, *J. Am. Chem. Soc.*, 2005, **127**, 17998–17999; (*b*) H. Furukawa, M. A. Miller and O. M. Yaghi, *J. Mater. Chem.*, 2007, **17**, 3197–3204; (*c*) H. Chun, H. Jung and J. Seo, *Inorg. Chem.*, 2009, **48**, 2043–2047.

9 (*a*) G. Yang, R. G. Raptis and P. Šafár, *Cryst. Growth Des.*, 2008, **8**, 981–985; (*b*) D. L. Long, A. J. Blake, N. R. Champness, C. Wilson and M. Schröder, *J. Am. Chem. Soc.*, 2001, **123**, 3401–3402.

10 (*a*) C. Qin, X. L. Wang, E. B. Wang and Z. M. Su, *Inorg. Chem.*, 2005, **44**, 7122–7129; (*b*) K. Z. Shao, Y. H. Zhao, X. L. Wang, Y. Q. Lan, D. J. Wang, Z. M. Su and R. S. Wang, *Inorg. Chem.*, 2009, **48**, 10–12.

11 (*a*) M. C. Hong, Y. J. Zhao, W. P. Su, R. Cao, M. Fujita, Z. Y. Zhou and A. S. C. Chan, *Angew. Chem., Int. Ed.*, 2000, **39**, 2468–2470; (*b*) M. C. Hong, Y. J. Zhao, W. P. Su, R. Cao, M. Fujita, Z. Y. Zhou and A. S. C. Chan, *J. Am. Chem. Soc.*, 2000, **122**, 4819–4820.

12 A. J. Blake, N. R. Brooks, N. R. Champness, P. A. Cooke, A. M. Deveson, D. Fenske, P. Hubberstey, W. S. Li and M. Schroder, *J. Chem. Soc., Dalton Trans.*, 1999, 2103–2110.

13 (*a*) S. Lopez, M. Kaharaman, M. Harmata and S. W. Keller, *Inorg. Chem.*, 1997, **36**, 6138–6140; (*b*) K. A. Hirsh, S. R. Wilson and J. S. Moore, *Inorg. Chem.*, 1997, **36**, 2960–2968.

14 (*a*) M. A. Withersby, A. J. Blake, N. R. Champness, P. A. Cooke, P. Hubberstey, W. S. Li and M. Schroder, *Inorg. Chem.*, 1999, **38**, 2259–2266; (*b*) T. L. Hennigar, D. C. MacQuarrie, P. Losier, R. D. Rogers and M. J. Zaworotko, *Angew. Chem., Int. Ed. Engl.*, 1997, **36**, 972–973.

15 (*a*) M. A. Withersby, A. J. Blake, N. R. Champness, P. Hubberstey, W. S. Li and M. Schroder, *Angew. Chem., Int. Ed. Engl.*, 1997, **36**, 2327–2329; (*b*) L. Carlucci, G. Ciani, P. Macchi, D. M. Proserpio and S. Rizaato, *Chem. – Eur. J.*, 1999, **5**, 237–243; (*c*) J. R. Black, N. R. Champness, W. Levason and G. J. Reid, *J. Chem. Soc., Chem. Commun.*, 1995, 1277–1278; (*d*) J. R. Black, N. R. Champness, W. Levason and G. Reid, *J. Chem. Soc., Dalton Trans.*, 1995, 3439–3445.

16 (*a*) Z. L. Chen, Y. F. Wang, L. Liu, Z. Zhang and F. P. Liang, *Chem. Commun.*, 2012, **48**, 11689–11691; (*b*) B. Wisser, A. C. Chamayou, R. Miller, W. Scherer and C. Janiak, *CrystEngComm*, 2008, **10**, 461–464; (*c*) D. Sun, D. F. Wang, F. J. Liu, H. J. Hao, N. Zhang, R. B. Huang and L. S. Zheng, *CrystEngComm*, 2011, **13**, 2833–2836; (*d*) A. A. Khandar, F. A. Afkhami, S. A. H. Yazdi, J. M. White, S. Kassel, W. G. Dougherty, J. Lipkowski, D. Van Derveer, G. Giester and F. Costantino, *Inorg. Chim. Acta*, 2015, **427**, 87–96.

17 (*a*) M. Chakrabarti, E. Munck and E. L. Bominaar, *Inorg. Chem.*, 2011, **50**, 4322–4326; (*b*) E. L. M. Wong, R. W. Y. Sun, N. P. Y. Chung, C. L. S. Lin, N. Y. Zhu and C. M. Che, *J. Am. Chem. Soc.*, 2006, **128**, 4938–4939; (*c*) Y. S. Moroz, K. Kulon, M. Haukk, E. Gumienna-Kontecka, H. Kozłowski, F. Meyer and I. O. Fritsky, *Inorg. Chem.*, 2008, **47**, 5656–5665; (*d*) D. J. D. Wilson, C. M. Beavers and A. F. Richards, *Eur. J. Inorg. Chem.*, 2012, 1130–1138; (*e*) H. Xiang, Y. H. Lan, L. Jiang, W. X. Zhang, C. E. Anson, T. B. Lu and A. K. Powell, *Inorg. Chem. Commun.*, 2012, **16**, 51–54.

18 (*a*) M. Fujita, D. Oguro, M. Miyazawa, H. Oka, K. Yamaguchi and K. Ogura, *Nature*, 1995, **378**, 469–471; (*b*) S. R. Batten and R. Robson, *Angew. Chem., Int. Ed.*, 1998, **37**, 1460–1494; (*c*) H. Okamoto and M. Yamashita, *Bull. Chem. Soc. Jpn.*, 1998, **71**, 2023–2039; (*d*) A. A. Khandar, F. A. Afkhami, S. A. Hosseini-Yazdi, J. Lipkowski, W. G. Dougherty, W. S. Kassel, H. R. Prieto and S. G. Granda, *J. Inorg. Organomet. Polym.*, 2015, **25**, 860–868.

19 (*a*) C. J. Matthews, L. K. Thompson, S. R. Parsons, Z. Xu, D. O. Miller and S. L. Heath, *Inorg. Chem.*, 2001, **40**, 4448–4454; (*b*) L. K. Thompson, *Coord. Chem. Rev.*, 2002, **233–234**, 193–206; (*c*) Z. Xu, L. K. Thompson and D. O. Miller, *J. Chem. Soc., Dalton Trans.*, 2002, 2462–2466.

20 (*a*) S. Yumnam and L. Rajkumari, *J. Chem. Eng. Data*, 2009, **54**, 28; (*b*) A. A. Khandar, B. K. Ghosh, C. Lampropoulos, M. S. Gargari, V. T. Yilmaz, K. Bhar, S. A. Hosseini-Yazdi, J. M. Cain and G. Mahmoudi, *Polyhedron*, 2015, **85**, 467–475.

21 (*a*) M. Abedi, O. Z. Yesilel, G. Mahmoudi, A. Bauza, S. E. Lofland, Y. Yerli, W. Kaminsky, P. Garczarek, J. K. Zareba, A. Ienco, A. Frontera and M. S. Gargari, *Inorg. Chim. Acta*, 2016, **443**, 101–109; (*b*) G. Mahmoudi, A. Bauzá, A. V. Gurbanov, F. I. Zubkov, W. Maniukiewicz, A. Rodríguez-Diéguez, E. López-Torres and A. Frontera, *CrystEngComm*, 2016, **18**, 9056–9066.

22 G. M. Sheldrick, *SHELXTL: Structure Determination Software Suite, Version 6.14*, Bruker AXS, Madison, WI, USA, 2003.

23 L. J. Farrugia, *J. Appl. Crystallogr.*, 1999, **32**, 837–838.

24 Mercury, version 3.0; CCDC, available online via ccdc.cam.ac.uk/products/mercury.

25 A. L. Spek, *PLATON-a multipurpose crystallographic tool*, Utrecht University, Utrecht, 2005.

26 M. A. Spackman and D. Jayatilaka, *CrystEngComm*, 2009, **11**, 19–32.

27 M. A. Spackman and J. J. McKinnon, *CrystEngComm*, 2002, **4**, 378–392.

28 S. K. Wolff, D. J. Grimwood, J. J. McKinnon, M. J. Turner, D. Jayatilaka and M. A. Spackman, *CrystalExplorer (Version 3.1)*, University of Western Australia, 2012.

29 M. J. Frisch, G. W. Trucks, H. B. Schlegel, G. E. Scuseria, M. A. Robb, J. R. Cheeseman, G. Scalmani, V. Barone, B. Mennucci, G. A. Petersson, H. Nakatsuji, M. Caricato, X. Li, H. P. Hratchian, A. F. Izmaylov, J. Bloino, G. Zheng, J. L. Sonnenberg, M. Hada, M. Ehara, K. Toyota, R. Fukuda, J. Hasegawa, M. Ishida, T. Nakajima, Y. Honda, O. Kitao, H. Nakai, T. Vreven, J. A. Montgomery Jr., J. E. Peralta, F. Ogliaro, M. Bearpark, J. J. Heyd, E. Brothers, K. N. Kudin, V. N. Staroverov, R. Kobayashi, J. Normand, K. Raghavachari, A. Rendell, J. C. Burant, S. S. Iyengar, J. Tomasi, M. Cossi, N. Rega, J. M. Millam, M. Klene, J. E. Knox, J. B. Cross, V. Bakken, C. Adamo, J. Jaramillo, R. Gomperts, R. E. Stratmann, O. Yazyev, A. J. Austin, R. Cammi, C. Pomelli, J. W. Ochterski, R. L. Martin, K. Morokuma, V. G. Zakrzewski, G. A. Voth, P. Salvador, J. J. Dannenberg, S. Dapprich, A. D. Daniels, Ö. Farkas, J. B. Foresman, J. V. Ortiz, J. Cioslowski and D. J. Fox, *Gaussian 09, Revision B.01*, Gaussian, Inc., Wallingford CT, 2009.

30 S. Grimme, J. Antony, S. Ehrlich and H. Krieg, *J. Chem. Phys.*, 2010, **132**, 154104–154123.

31 T. A. Keith, *AIMAll (Version 13.05.06)*, TK Gristmill Software, Overland Park KS, USA, 2013.

32 M. Rademeyer, C. Tsouris, D. G. Billing, A. Lemmerer and J. Charmant, *CrystEngComm*, 2011, **13**, 3485–3497.

33 J. Martí-Rujas and M. Cametti, *New J. Chem.*, 2014, **38**, 1385–1388.

34 (*a*) G. Mínguez-Espallargas, F. Zordan, L. Arroyo-Marín, H. Adams, K. Shankland, J. van de Streek and L. Brammer, *Chem. – Eur. J.*, 2009, **15**, 7554–7568; (*b*) L. Dobrzycki and K. Woźniak, *J. Mol. Struct.*, 2009, **921**, 18–33; (*c*) E. C. Constable, G. Zhang, C. E. Housecroft, M. Neuburger and J. A. Zampese, *CrystEngComm*, 2010, **12**, 2146–2152; (*d*) E. V. Savinkina, E. A. Buravlev, I. A. Zamilatskov, D. V. Albov, V. V. Kravchenko, M. G. Zaitseva and B. N. Mavrin, *Z. Anorg. Allg. Chem.*, 2009, **635**, 1458–1462; (*e*) W. Petz and B. Neumüller, *Eur. J. Inorg. Chem.*, 2011, **2011**, 4889–4895; (*f*) A. Stasch, *Chem. – Eur. J.*, 2012, **18**, 15105–15112.

35 (*a*) A. K. Tewari and R. Dubey, *Bioorg. Med. Chem.*, 2008, **16**, 126–143; (*b*) P. Mignon, S. Loverix, J. Steyaert and P. Geerlings, *Nucleic Acids Res.*, 2005, **33**, 1779–1789; (*c*) J. Sponer, K. E. Riley and P. Hobza, *Phys. Chem. Chem. Phys.*, 2008, **10**, 2595–2610; (*d*) X. J. Wang, L. C. Gui, Q. L. Ni, Y. F. Liao, X. F. Jiang, L. H. Tang, L. H. Zhang and Q. Wu, *CrystEngComm*, 2008, **10**, 1003–1010; (*e*) S. L. Cockroft, C. A. Hunter, K. R. Lawson, J. Perkins and C. J. Urch, *J. Am. Chem. Soc.*, 2005, **127**, 8594–8595; (*f*) T. Sato, T. Tsuneda and K. Hirao, *J. Chem. Phys.*, 2005, **123**, 104307–104317; (*g*) S. Grimme, *Angew. Chem., Int. Ed.*, 2008, **47**, 3430–3434; (*h*) M. Rubeš, O. Bludsky' and P. Nachtigall, *ChemPhysChem*, 2008, **9**, 1702–1708; (*i*) E. C. Lee, D. Kim, P. Jurecka, P. Tarakeshwar, P. Hobza and K. S. Kim, *J. Phys. Chem. A*, 2007, **111**, 3446–3457; (*j*) M. O. Sinnokrot and C. D. Sherrill, *J. Phys. Chem. A*, 2006, **110**, 1065610668; (*k*) R. Podeszwa, R. Bukowski and K. Szalewicz, *J. Phys. Chem. A*, 2006, **110**, 10345–10354; (*l*) M. Pitonak, P. Neogrady, J. Rezac, P. Jurecka, M. Urban and P. Hobza, *J. Chem. Theory Comput.*, 2008, **4**, 1829–1834.

36 (*a*) B. D. Ostojić, G. V. Janjić and S. D. Zarić, *Chem. Commun.*, 2008, 6546–6548; (*b*) Z. D. Tomić, S. B. Novaković and S. D. Zarić, *Eur. J. Inorg. Chem.*, 2004, **11**, 2215–2218; (*c*) D. N. Sredojević, Z. D. Tomić and S. D. Zarić, *Cent. Eur. J. Chem.*, 2007, **5**, 20–31; (*d*) Z. D. Tomić, D. N. Sredojević and S. D. Zarić, *Cryst. Growth Des.*, 2006, **6**, 29–31; (*e*) D. N. Sredojević, G. A. Bogdanović, Z. D. Tomić and S. D. Zarić, *CrystEngComm*, 2007, **9**, 793–798; (*f*) A. Castineiras, A. G. Sicilia-Zafra, J. M. Gonzales-Perez, D. Choquesillo-Lazarte and J. Niclos-Gutierrez, *Inorg. Chem.*, 2002, **41**, 6956–6958; (*g*) E. Craven, C. Zhang, C. Janiak, G. Rheinwald and H. Lang, *Z. Anorg. Allg. Chem.*, 2003, **629**, 2282–2290; (*h*) U. Mukhopadhyay, D. Choquesillo-Lazarte, J. Niclos-Gutierrez and I. Bernal, *CrystEngComm*, 2004, **6**, 627–632; (*i*) D. Pucci, V. Albertini, R. Bloise, A. Bellusci, A. Cataldi, C. V. Catapano, M. Ghedini and A. Crispini, *J. Inorg. Biochem.*, 2006, **100**, 1575–1578; (*j*) S. P. Mosae, E. Suresh and P. S. Subramanian, *Polyhedron*, 2009, **28**, 245–252; (*k*) X. J. Wang, H. X. Jian, Z. P. Liu, Q. L. Ni, L. C. Gui and L. H. Tang, *Polyhedron*, 2008, **27**, 2634–2642; (*l*) S.

Chowdhury, M. G. B. Drew and D. Datta, *Inorg. Chem. Commun.*, 2003, **6**, 1014–1016; (*m*) X. Wang, O. V. Sarycheva, B. D. Koivisto, A. H. McKie and F. Hof, *Org. Lett.*, 2008, **100**, 297–300.

37 (*a*) H. Masui, *Coord. Chem. Rev.*, 2001, **219–221**, 957–992; (*b*) M. K. Milčić, B. D. Ostojić and S. D. Zarić, *Inorg. Chem.*, 2007, **46**, 7109–7114.

38 R. F. W. Bader, *Chem. Rev.*, 1991, **91**, 893–928.

39 (*a*) A. Bauzá and A. Frontera, *Angew. Chem., Int. Ed.*, 2015, **54**, 7340–7343; (*b*) S. Jana, S. Khan, A. Bauzá, A. Frontera and S. Chattopadhyay, *J. Mol. Struct.*, 2017, **1127**, 355–360.

40 M. O. Sinnokrot, E. F. Valeev and C. D. Sherrill, *J. Am. Chem. Soc.*, 2002, **124**, 10887–10893.